

μ_2, η^1 -*N*-[(*N,N*-Dimethylamino)dimethylsilyl]-2,6-diisopropylanilido Metal (Li, Zr, Hf) Compounds and the Catalytic Behaviors of the IVB Compounds in Ethylene (Co)Polymerization[‡]

Shifang Yuan,^{†,‡} Xuehong Wei,[†] Hongbo Tong,[†] Liping Zhang,^{†,‡} Diansheng Liu,^{*,†} and Wen-Hua Sun^{*,‡}

[†]Institute of Applied Chemistry, Shanxi University, Taiyuan 030006, People's Republic of China, and

[‡]Key Laboratory of Engineering Plastics and Beijing National Laboratory for Molecular Sciences, Institute of Chemistry, Chinese Academy of Sciences, Beijing 100190, People's Republic of China

Received January 20, 2010

The dimer of lithium μ_2, η^1 -*N*-[(*N,N*-dimethylamino)dimethylsilyl]-2,6-diisopropylanilidate [**1c**, $[\text{LiN}(2,6\text{-}i\text{Pr}_2\text{C}_6\text{H}_3)\text{Si}(\text{CH}_3)_2\text{N}(\text{CH}_3)_2]_2$] represented as $(\text{LiL})_2$] reacted with group 4 chlorides to form corresponding compounds, which were crystallized and confirmed by X-ray diffraction analysis as compounds of pseudotetrahedral ZrL_2Cl_2 (**2**) and chloro-bridged dinuclear tetrahedral compounds $\text{ZrLCl}_2(\mu\text{-Cl})_2\text{Li}\cdot 2\text{THF}$ (**3**), $\text{ZrLCl}_2(\mu\text{-Cl})_2\text{Li}\cdot 2\text{Et}_2\text{O}$ (**4**), $\text{HfLCl}_2(\mu\text{-Cl})_2\text{Li}\cdot 2\text{Et}_2\text{O}$ (**5**), and $[\text{ZrLCl}_2(\mu\text{-Cl})_2]$ (**6**). The catalytic behaviors of group 4 compounds were investigated in the presence of MAO as a cocatalyst. Compound **4** exhibited high activity for ethylene polymerization, while compounds **2** and **6** showed good activities for both ethylene polymerization and ethylene/1-hexene copolymerization.

Introduction

Organoamidolithium compounds have been extensively studied for their reactivities and transformation of organo-amido-metal compounds,¹ in which some of them provide efficient procatalysts in olefin polymerization.² In trials of organometallic procatalysts for olefin polymerization,³ the

IVB compounds have been extensively explored such as metallocene derivatives⁴ and half-metallocene derivatives;⁵ moreover, the so-called constrained-geometry catalysts (CGC) of the half-metallocene compounds were finally commercialized.⁶ Recently the nonbridged half-metallocene compounds were found to show high efficiency both in catalytic activity and in precisely controlling copolymer properties.⁷ In addition, the bis(imino)titanium compounds performed with high activities toward either ethylene polymerization or ethylene copolymerization with α -olefins.⁸ The catalytic behavior of transition metal compounds bearing the silylamido motifs⁹ acting as versatile ligands in various reactive patterns¹⁰ has been widely explored.¹¹ In our recent work regarding silylamidolithium and group 4 metal compounds,¹² the highly sensitive μ_2, η^1 -*N*-[(*N,N*-dimethylamino)dimethylsilyl]-2,6-diisopropylanilidometal (Li, Zr, Hf)

[‡] Dedicated to Prof. Dr. Uwe Rosenthal of the University of Rostock, Germany, on the occasion of his 60th birthday.

*Corresponding authors. Tel: +86-10-62557955. Fax: +86-10-62618239. E-mail: whsun@iccas.ac.cn (W.-H.S.); dsliu@sxu.edu.cn (D.L.).

(1) Lappert, M. F.; Power, P. P.; Sanger, A. R.; Srivastava, R. C. *Metal and Metalloid Amides*; Ellis Horwood Ltd.: England, 1980.

(2) (a) Guram, A. S.; Jordan, R. F. In *Comprehensive Organometallic Chemistry II*; Lappert, M. F., Ed.; Elsevier Scientific Ltd: Oxford, 1995; Vol. 4, p 589. (b) Bochmann, M. *J. Chem. Soc., Dalton Trans.* **1996**, 255. (c) Brintzinger, H. H.; Fischer, D.; Müllhaupt, R.; Rieger, B.; Waymouth, R. M. *Angew. Chem., Int. Ed. Engl.* **1995**, *34*, 1143. (d) McKnight, A. L.; Waymouth, R. M. *Chem. Rev.* **1998**, *98*, 2587. (e) Resconi, L.; Cavallo, L.; Fait, A.; Piemontesi, F. *Chem. Rev.* **2000**, *100*, 1253.

(3) (a) Ziegler, K.; Gellert, H. G.; Zosel, K.; Lehmkuhl, W.; Pfohl, W. *Angew. Chem.* **1955**, *67*, 424. (b) Ziegler, K.; Holzkamp, E.; Breil, H.; Martin, H. *Angew. Chem.* **1955**, *67*, 541. (c) Natta, G. *J. Polym. Sci.* **1955**, *16*, 143. (d) Natta, G.; Pino, P.; Corradini, P.; Danusso, F.; Mantica, E.; Mazzanti, G.; Moraglio, G. *J. Am. Chem. Soc.* **1955**, *77*, 1708. (e) Groppo, E.; Lambert, C.; Bordiga, S.; Spoto, G.; Zecchina, A. *Chem. Rev.* **2005**, *105*, 115.

(4) (a) Sinn, H.; Kaminsky, W.; Vollmer, H.-J.; Woldt, R. *Angew. Chem., Int. Ed. Engl.* **1980**, *19*, 390. (b) Kaminsky, W. *Macromol. Chem. Phys.* **1996**, *197*, 3907. (c) Brintzinger, H. H.; Fischer, D.; Müllhaupt, R.; Rieger, B.; Waymouth, R. M. *Angew. Chem., Int. Ed. Engl.* **1995**, *34*, 1143. (d) Alt, H. G.; Köppl, A. *Chem. Rev.* **2000**, *100*, 1205.

(5) McKnight, A. L.; Waymouth, R. M. *Chem. Rev.* **1998**, *98*, 2587.

(6) (a) Stevens, J. C.; Timmers, F. J.; Wilson, D. R.; Schmidt, G. F.; Nickias, P. N.; Rosen, R. K.; McKnight, G. W.; Lai, S. Eur. Pat. Appl. 0416815A2, **1991**. (b) Shapiro, P. J.; Bunel, E.; Schaefer, W. P.; Bercaw, J. E. *Organometallics* **1990**, *9*, 867. (c) Shapiro, P. J.; Cotter, W. D.; Schaefer, W. P.; Labinger, J. A.; Bercaw, J. E. *J. Am. Chem. Soc.* **1994**, *116*, 4623.

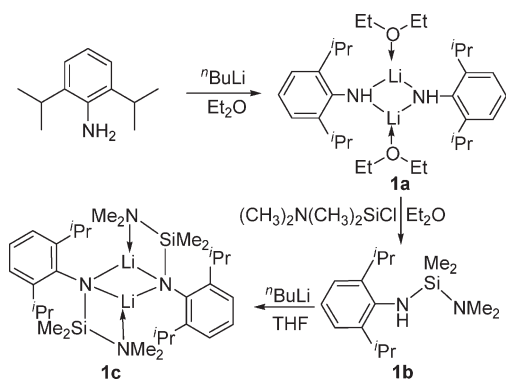
(7) (a) Nomura, K. *Dalton Trans.* **2009**, 8811. (b) Nomura, K.; Liu, J.; Padmanabhan, S.; Kitiyanan, B. *J. Mol. Catal. A: Chem.* **2007**, *267*, 1. (c) Liu, S.; Yi, J.; Zuo, W.; Wang, K.; Wang, D.; Sun, W.-H. *J. Polym. Sci., Part A: Polym. Chem.* **2009**, *47*, 3154. (d) Zuo, W.; Zhang, S.; Liu, S.; Liu, X.; Sun, W.-H. *J. Polym. Sci., Part A: Polym. Chem.* **2008**, *46*, 3396. (e) Liu, S.; Zuo, W.; Zhang, S.; Hao, P.; Wang, D.; Sun, W.-H. *J. Polym. Sci., Part A: Polym. Chem.* **2008**, *46*, 3411.

(8) (a) Matsugi, T.; Fujita, T. *Chem. Soc. Rev.* **2008**, *37*, 1264. (b) Yoshida, Y.; Matsui, S.; Takagi, Y.; Mitani, M.; Nakano, T.; Tanaka, H.; Kashiwa, N.; Fujita, T. *Organometallics* **2001**, *20*, 4793. (c) Yoshida, Y.; Mohri, J.; Ishii, S.; Mitani, M.; Saito, J.; Matsui, S.; Makio, H.; Nakano, T.; Tanaka, H.; Onda, M.; Yamamoto, Y.; Mizuno, A.; Fujita, T. *J. Am. Chem. Soc.* **2004**, *126*, 12023. (d) Zuo, W.; Sun, W.-H.; Zhang, S.; Hao, P.; Shiga, A. *J. Polym. Sci., Part A: Polym. Chem.* **2007**, *45*, 3415.

(9) Braunschweig, H.; Breitling, F. M. *Coord. Chem. Rev.* **2006**, *250*, 2691.

(10) (a) Chomitz, W. A.; Arnold, J. *Chem. Commun.* **2007**, 4797. (b) Ferreira, H.; Dias, A. R.; Duarte, M. T.; Ascenso, J. R.; Martins, A. M. *Inorg. Chem.* **2007**, *46*, 750. (c) Passarelli, V.; Benetollo, F.; Zanella, P. *Eur. J. Inorg. Chem.* **2004**, 1714.

Scheme 1. Synthesis of Ligands 1a–c

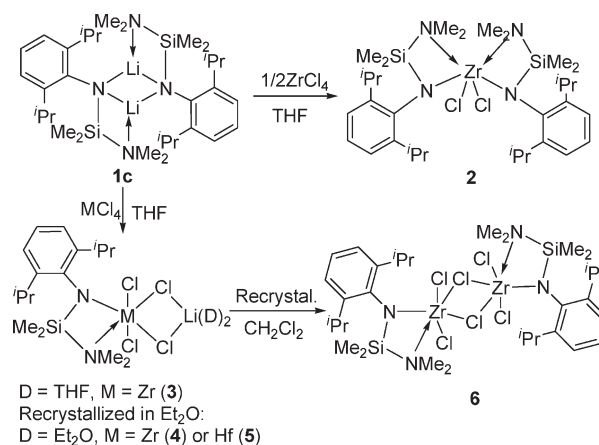


compounds were prepared and structurally confirmed. These Zr and Hf compounds show good activities toward ethylene (co)polymerization. Here we report the synthesis and characterization of such NSiN chelate complexes in detail and describe the catalytic activities of the Zr and Hf compounds toward ethylene (co)polymerizations.

Results and Discussion

Synthesis and Characterization. The reactions of N -substituted anilines with lithium derivatives commonly formed anilidolithium dimers.¹³ The potassium hydrido-anilidate, without evidence of crystal structure, was proposed as a reactive intermediate in organic synthesis.¹⁴ Although the acidic properties of the $N\text{-H}$ are observed, the stoichiometric reaction of 2,6-diisopropylaniline with $n\text{-BuLi}$ quantitatively formed the dimeric lithium anilide $[\text{LiNH}(2,6\text{-}i\text{Pr}_2\text{C}_6\text{H}_3) \cdot \text{Et}_2\text{O}]_2$ (**1a**), with an isolated yield of 97%. Further treatment of $[\text{LiNH}(2,6\text{-}i\text{Pr}_2\text{C}_6\text{H}_3) \cdot \text{Et}_2\text{O}]_2$ (**1a**) with two equivalents of $(\text{CH}_3)_2\text{N}(\text{CH}_3)_2\text{SiCl}$ in Et_2O quantitatively produced the compound $(\text{CH}_3)_2\text{N}(\text{CH}_3)_2\text{SiNH}(2,6\text{-}i\text{Pr}_2\text{C}_6\text{H}_3)$ (**HL**, **1b**). The stoichiometric reaction of $(\text{CH}_3)_2\text{N}(\text{CH}_3)_2\text{SiNH}(2,6\text{-}i\text{Pr}_2\text{C}_6\text{H}_3)$ (**HL**, **1b**) with $n\text{-BuLi}$ in tetrahydrofuran (THF) gave the μ_2, η^1 - N -[(N,N -dimethylamino)dimethylsilyl]-2,6-diisopropylanilido lithium dimer [(LiL) $_2$, **1c**]. The synthetic procedure of compounds **1a–c** is illustrated

Scheme 2. Synthesis of the Metal Compounds 2–6



in Scheme 1, and all newly synthesized compounds were characterized by elemental analyses and NMR spectra, and by single-crystal X-ray diffraction for colorless crystals of **1a** and **1c**.

The lithium μ_2, η^1 - N -[(N,N -dimethylamino)dimethylsilyl]-2,6-diisopropylanilido dimer (**1c**) reacted with appropriate amounts of Zr or Hf chlorides to form corresponding metal compounds (**2–6**) (Scheme 2). The reaction of 2 equiv of **1c** to zirconium tetrachloride in THF resulted in a light-colored solution, which was extracted into toluene and crystallized at $-20\text{ }^\circ\text{C}$ to provide colorless crystals of ZrL_2Cl_2 (**2**) in a nice yield. Reactions with a ligand/metal ratio of 1:1 gave compounds of which the molecular structures showed solvent molecules used in crystallization. For zirconium, the extracted solution of toluene/THF (4:1) was crystallized at $-10\text{ }^\circ\text{C}$ to give red crystals of complex **3**, $\text{ZrLCl}_2(\mu\text{-Cl})_2\text{Li} \cdot 2\text{THF}$, which contains trichlorozirconium μ_2, η^1 - N -[(N,N -dimethylamino)dimethylsilyl]-2,6-diisopropylanilido and lithium chloride with two THF molecules. Using ether to extract metal compounds, both zirconium and hafnium compounds gave the analogous ether adducts $\text{MLCl}_2(\mu\text{-Cl})_2\text{Li} \cdot 2\text{Et}_2\text{O}$ (M = Zr, **4**; M = Hf, **5**). Meanwhile using dichloromethane to extract the zirconium compound for crystallization at $-10\text{ }^\circ\text{C}$, dimer **6**, $[\text{ZrLCl}_2(\mu\text{-Cl})_2]$, was isolated in good yield. Unlike compounds **3–5** crystallized with an adduct of LiCl, the dichloromethane provided the chloro interaction with zirconium for cleaving lithium chloride, and two cationic zirconium units aggregated through bridging chlorides as dimer **6** in the solid state. The synthetic procedures and transformation of compounds **2–6** are illustrated in Scheme 2.

Crystal Structures. X-ray diffraction analysis indicated that the compound $[(2,6\text{-}i\text{Pr}_2\text{C}_6\text{H}_3)\text{HN Li} \cdot \text{Et}_2\text{O}]_2$, **1a**, crystallized as a centrosymmetric dimer with a planar Li_2N_2 core (Figure 1) with its bond lengths and angles collected in Table S1 of the Supporting Information. The lithium atoms are bonded to two bridging NHAr groups with one coordinated Et_2O molecule per lithium. The Li–N distances (1.997(6)–2.020(6) Å) were normal between the Li–N distances within 1.961–1.962 Å^{13a} and 2.01–2.18 Å.^{15–19} The

(11) (a) Bambirra, S.; Meetsma, A.; Hessen, B. *Organometallics* **2006**, *25*, 3486. (b) Morello, L.; Yu, P. H.; Carmichael, C. D.; Patrick, B. O.; Fryzuk, M. D. *J. Am. Chem. Soc.* **2005**, *127*, 12796. (c) Kim, S.-J.; Jung, I. N.; Yoo, B. R.; Cho, S.; Ko, J.; Kim, S. H.; Kang, S. O. *Organometallics* **2001**, *20*, 1501. (d) Kim, S.-J.; Jung, I. N.; Yoo, B. R.; Kim, S. H.; Ko, J.; Byun, D.; Kang, S. O. *Organometallics* **2001**, *20*, 2136. (e) Kim, S.-J.; Lee, Y.-J.; Kim, S. H.; Ko, J.; Cho, S.; Kang, S. O. *Organometallics* **2002**, *21*, 5358. (f) Barroso, S.; Cui, J. L.; Dias, A. R.; Duarte, M. T.; Ferreira, H.; Henriques, R. T.; Oliveira, M. C.; Ascenso, J. R.; Martins, A. M. *Inorg. Chem.* **2006**, *45*, 3532. (g) Passarelli, V.; Benetollo, F.; Zanella, P.; Carta, G.; Rossetto, G. *Dalton Trans.* **2003**, 1411. (h) Chomitz, W. A.; Minasian, S. G.; Sutton, A. D.; Arnold, J. *Inorg. Chem.* **2007**, *46*, 7199. (i) Brauer, D. J.; Bürger, H.; Liewald, G. R.; Wilke, J. *J. Organomet. Chem.* **1986**, *310*, 317. (j) Veith, M.; Frank, W.; Töllner, F.; Lange, H. *J. Organomet. Chem.* **1987**, *326*, 315. (k) Horton, A. D.; With, J. *Organometallics* **1997**, *16*, 5424. (l) Shattenmann, F. J.; Schrock, R. R.; Davis, W. M. *Organometallics* **1998**, *17*, 989. (m) Schumann, H.; Gottfriedsen, J.; Dechert, S.; Girgsdies, F. *Z. Anorg. Allg. Chem.* **2000**, *626*, 747. (n) Hill, M. S.; Hitchcock, P. B. *Organometallics* **2002**, *21*, 3258.

(12) (a) Bai, S.-D.; Tong, H. B.; Guo, J. P.; Zhou, M.-S.; Liu, D.-S.; Yuan, S.-F. *Polyhedron* **2010**, *29*, 262. (b) Zhou, M. S.; Zhang, S.; Tong, H. B.; Sun, W.-H.; Liu, D.-S. *Inorg. Chem. Commun.* **2007**, *10*, 1262.

(13) (a) Kennepohl, D. K.; Brooker, S.; Sheldrick, G. M.; Roesky, H. W. *Chem. Ber.* **1991**, *124*, 2223. (b) Ren, G. M.; Shang, D. L.; Guo, J. P. *Acta Crystallogr. E* **2007**, *E63*, m793.

(14) (a) Turaeva, D. A.; Kurbatov, Y. V. *Russ. J. Org. Chem.* **2004**, *38*, 1691. (b) Turaeva, D. A.; Kurbatov, Y. V. *Russ. J. Org. Chem.* **2004**, *40*, 1787.

(15) Cetinkaya, B.; Hitchcock, P. B.; Lappert, M. F.; Misra, M. C.; Thorne, A. J. *J. Chem. Soc., Chem. Commun.* **1984**, 148.

(16) Bartlett, R. A.; Chen, H.; Dias, H. V. R.; Olmstead, M. M.; Power, P. P. *J. Am. Chem. Soc.* **1988**, *110*, 446.

(17) Tang, Y. J.; Zakharov, L. N.; Rheingold, A. L.; Kemp, R. A. *Inorg. Chim. Acta* **2006**, *359*, 775.

(18) Cole, M. L.; Jones, C.; Junk, P. C. *New J. Chem.* **2002**, *26*, 89.

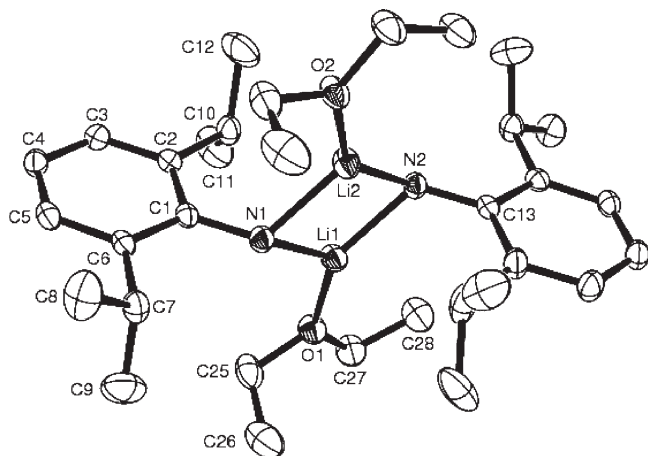


Figure 1. Molecular structure of compound **1a** with thermal ellipsoids at 30% probability. Hydrogen atoms have been omitted for clarity.

planar Li_2N_2 core formed a rhombus. It was also noted that an agostic interaction between Li and H atoms on the coordinated $\text{CH}(\text{CH}_3)_2$ was found in this molecule, based on a short $\text{Li}\cdots\text{H}$ distance of 2.220 Å, which was shorter than that in the related structure $[(\text{ad-Dipp})\text{NHLi}\cdot\text{Et}_2\text{O}]_2$ (2.32 Å).¹⁷

The molecular structure of compound **1c** formed a chair-type arrangement of three fused four-membered lithiocyclic rings with the central Li_2N_2 and two LiSiN_2 rings (Figure 2), and its bond lengths and angles are collected in Table S2 of the Supporting Information. The interplanar angle between the four-membered rings in the backbone of **1c** is 87.49°. Each lithium atom is bonded by three nitrogen atoms in the N_4Li_2 core, which gives rise to approximate trigonal-pyramidal geometry around both lithium atoms. Four atoms of two lithium and two nitrogen in the central Li_2N_2 ring are coplanar and form a rhombus with sides of 2.02 Å and $\text{Li}-\text{N}-\text{Li}'$ angles of 73.6(3)°. The $\text{Li}\cdots\text{Li}$ distance [2.419(11) Å] is longer than the previously reported $\text{Li}\cdots\text{Li}$ [2.397(11) Å] in $[\text{LiN}(\text{SiMe}_2\text{NMe}_2)(2,6\text{-Me}_2\text{C}_6\text{H}_3)]_2$,^{13b} shorter than that [2.465(7) Å] in **1a** and those [2.494(6)–2.521(7) Å] in $[(\text{XMe}_2\text{Si})_2\text{N}]_2\text{Li}_2$.^{20,21} The nitrogen donors in **1c** do effectively bind to lithium, so that the $\text{Li}-\text{N}$ bonding in the central ring is weakened and the $\text{Li}\cdots\text{Li}$ distance is increased. The dihedral angles between the aryl ring and the Li_2N_2 or LiSiN_2 ring are 78.48° and 70.74°, respectively. In addition, there were weak interactions between Li and other atoms because of relatively shorter distances observed for examples of $\text{Li}-\text{C}(1)$ (2.485(10) Å) and $\text{Li}-\text{H}(11a)$ (2.669 Å).

In the molecular structure of compound **2** (Figure 3) with its bond lengths and angles collected in Table S3 of the Supporting Information, the six-coordinate zirconium

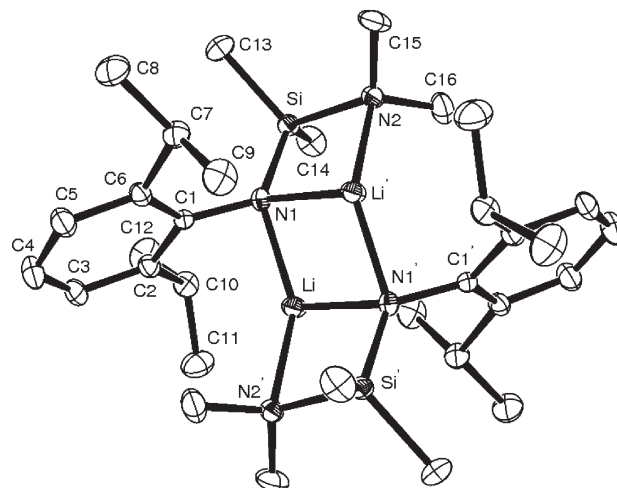


Figure 2. Molecular structure of compound **1c** with thermal ellipsoids at 30% probability. Hydrogen atoms have been omitted for clarity.

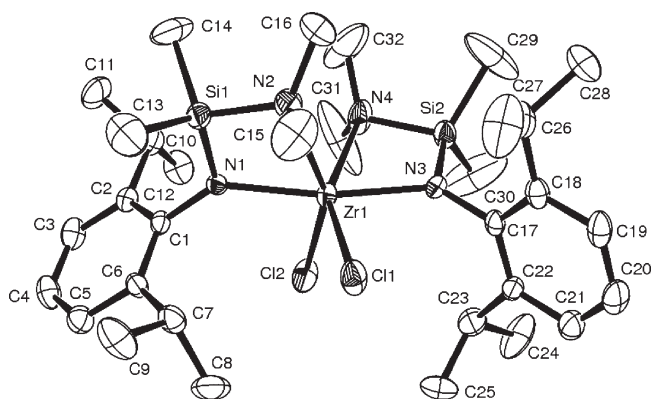


Figure 3. Molecular structure of compound **2** with thermal ellipsoids at 30% probability. Hydrogen atoms have been omitted for clarity.

center is located in an octahedral environment composed by two anionic $\mu_2,\eta^1\text{-N-}[(\text{N},\text{N-dimethylamino})\text{dimethylsilyl}]\text{-2,6-diisopropylanilidates}$, which were puckered rather than in a *trans* arrangement. The dihedral angle of planes $\text{N}(1)-\text{Zr}-\text{N}(2)$ and $\text{N}(3)-\text{Zr}-\text{N}(4)$ is 86.41°; that of $\text{N}(1)-\text{Zr}-\text{N}(2)$ and $\text{N}(1)-\text{Si}-\text{N}(2)$ is 7.06° (average vertical distance from Si to the $\text{N}(1)-\text{Zr}-\text{N}(2)$ plane is ca. 0.143 Å). The distances between $\text{Zr}\cdots\text{Si}$ (3.0682(19)–3.0844(18) Å) are too long to form bonds, while the $\text{Zr}-\text{N}$ bond lengths [2.15 Å for $\text{Zr}-\text{N}(1)$ and $\text{Zr}-\text{N}(3)$, 2.50 Å for $\text{Zr}-\text{N}(2)$ and $\text{Zr}-\text{N}(4)$] indicated differences of direct or coordination bonds. The shorter $\text{Si}-\text{N}$ distances [1.71 Å for $\text{Si}-\text{N}(1)$ and 1.77 Å for $\text{Si}-\text{N}(2)$] show some double-bond character, indicating a nonconjugated $\mu_2,\eta^1\text{-N-Si-N}$ group. The aryl ring and ZrSiN_2 ring are approximately vertical, at 84.33°. An analogous situation was identified to take place with the average C_s symmetry zirconium compounds.^{11b}

The X-ray diffraction study showed that compounds **3–5** have a similar structure to the “ate” complex, and the molecular structure of compound **3** is illuminated in Figure 4, while the molecular structures of compounds **4** and **5** are shown in the Supporting Information, with Tables S4–S6 collecting the bond lengths and angles for compounds **3–5**, respectively. The metal (Zr or Hf) is six-coordinated as a

(19) Khvorosta, A.; Shutova, P. L.; Harmsa, K.; Lorbertha, J.; Sundermeyera, J.; Karlovb, S. S.; Zaitseva, G. S. *Z. Anorg. Allg. Chem.* **2004**, *630*, 885.

(20) (a) Veith, M.; Koban, A.; Fries, K.; Spaniol, P.; Elsasser, R.; Rammo, A.; Huch, V.; Kleinstaub, U. *Organometallics* **1998**, *17*, 2612. (b) Chen, H.; Ruth, A.; Bartlett, H. V.; Dias, R.; Olmstead, M. M.; Philip, P. P. *Inorg. Chem.* **1991**, *30*, 2487.

(21) (a) Antolini, F.; Hitchcock, P. B.; Lappert, M. F.; Merle, P. G. *Chem. Commun.* **2000**, 1301. (b) Bezombes, J. P.; Hitchcock, P. B.; Lappert, M. F.; Merle, P. G. *J. Chem. Soc., Dalton Trans.* **2001**, 816. (c) Engelhardt, L. M.; Jacobsen, G. E.; Junk, P. C.; Raston, C. L.; Skelton, B. W. *J. Chem. Soc., Dalton Trans.* **1988**, 1011.

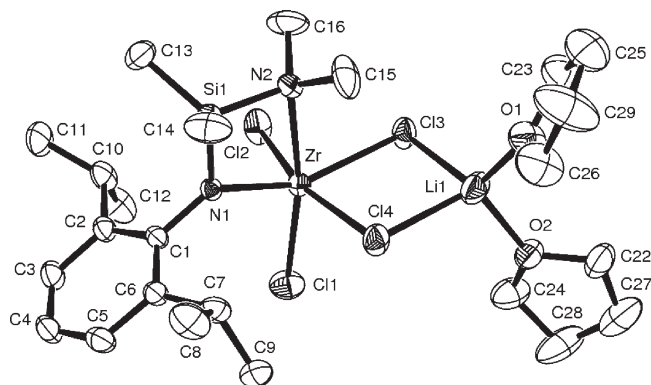


Figure 4. Molecular structure of compound **3** with thermal ellipsoids at 30% probability. Hydrogen atoms have been omitted for clarity.

distorted octahedron by one bidentate aminosilylamidate and four chlorides. The N–M–N angles of **2** [67.47(16)° and 68.05(17)°], **3** [69.64(11)°], **4** [69.51(13)°], and **5** [69.99(15)°] are far smaller than the right angle for an ideal octahedral geometry. As observed in compound **2**, the μ_2, η^1 -N–Si–N group is a nonconjugated group that forms one direct Zr–N bond [2.06 Å in both **3** and **4**] and one coordination Zr–N bond [2.41 Å in **3**, 2.44 Å in **4**], in which the direct Zr–N bond length is similar to the data [Zr–N 2.05–2.12 Å] for [HC(Me₂SiNR)₃Zr(μ -Cl)₂Li(Et₂O)₂].²² The distances of Zr···Si [3.0150(15) Å, **3**; 3.0071(15) Å, **4**] prove no interaction between them. Similar structural features are observed in compound **5**. The dihedral angles N(1)–Zr–N(2) and N(1)–Si–N(2) in **3** are 0.36°, meaning N(1)–Zr–N(2)–Si is virtually coplanar. The dihedral angles N(1)–M–N(2) and N(1)–Si–N(2) are 13.79° in **4** and 13.74° in **5** (average vertical distance from Si to the plane N(1)–M–N(2) is ca. 0.287 Å in **4** and ca. 0.285 Å in **5**).

The molecular structure of dinuclear zirconium compound [ZrLCl₂(μ -Cl)]₂ (**6**) consists of a discrete centrosymmetric center (Figure 5), with its bond lengths and angles collected in Table S7 of the Supporting Information. The association interactions between two zirconium atoms are four common bridging zirconium–chlorine bonds [2.5736(11)–2.6997(11) Å].^{23–26} Each zirconium unit is six-coordinated and possesses a distorted octahedral geometry. The benzylamido nitrogen atom and the bridging chloride ion occupy the axial sites N(1)–Zr–Cl(3) [158.54(9)°]. The main distortion results from the acute angle Cl(3)–Zr–Cl(3') [74.15(3)°] in the planar bridging Zr₂Cl₂ core, while the amino ligand chelating angle N(1)–Zr–N(2) [70.58(11)°] as well as the other bond angles around the zirconium center are within the usual ranges. The Zr–N direct bond [2.023(3) Å] and coordination bond [2.394(3) Å] in **6** are shorter than the corresponding values for **2–4**; however, the bond lengths of N–Si [1.738(3)–1.806(3) Å] in **6** are longer than those

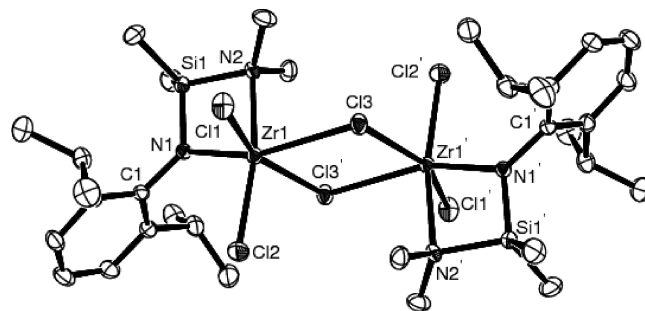


Figure 5. Molecular structure of compound **6** with thermal ellipsoids at 30% probability. Hydrogen atoms have been omitted for clarity.

observed in the above compounds (1.717(5)–1.775(5) Å in **2**, 1.724(3)–1.778(3) Å in **3**, and 1.727(4)–1.789(4) Å in **4**). The dihedral angle between planes N(1)–Zr–N(2) and N(1)–Si–N(2) is 10.78°. The plane N(1)–Si–N(2)–Zr is nearly perpendicular to the Zr₂Cl₂ plane with a dihedral angle of 87.61°, and the dihedral angle between the aryl ring and N(1)–Si–N(2)–Zr is 88.54°. As a consequence, the aryl rings and the Zr₂Cl₂ plane formed a small dihedral angle of 29.83°.

Catalytic Behavior of the Procatalysts 2 and 4–6. The compounds **2**, **4**, **5**, and **6** were investigated for their catalytic behaviors of ethylene (co)polymerization. The procatalyst **4** was studied for optimum conditions (entries 1–13 in Table 1). AlEt₃ or Et₂AlCl as activator gave little activity for ethylene polymerization (entries 1, 2 in Table 1). Using 1000 molar ratios of Al to Zr under ambient pressure of ethylene at 30 °C, the activities observed for ethylene polymerization were 1.30×10^4 g·mol(Zr)⁻¹·h⁻¹·atm⁻¹ for MMAO (entry 3 in Table 1) and 2.10×10^4 g·mol(Zr)⁻¹·h⁻¹·atm⁻¹ for MAO (entry 4 in Table 1). Employing 1000 equiv of MAO, the optimum reaction temperature at 1 bar was 50 °C (entries 4–6 in Table 1), and the best performance was 2.70×10^4 g·mol(Zr)⁻¹·h⁻¹·atm⁻¹ with the resulting polyethylene (PE) having a molecular weight of 337 kg·mol⁻¹ and a broad polydispersity (15) (entry 5 in Table 1). When the ethylene pressure was increased to 10 atm, both catalytic activities and the molecular weight of resultant PEs were enhanced (entries 7–13 in Table 1). Under 10 atm of ethylene pressure at 30 °C, the optimum Al/Zr ratio was 1000 (entry 8 in Table 1). Increasing the reaction temperature from 30 to 80 °C gave the highest activity of 1.73×10^5 g·mol(Zr)⁻¹·h⁻¹·atm⁻¹ at 70 °C (entry 12 in Table 1). Similarly, the hafnium procatalyst **5** also showed the highest activity of 2.40×10^4 g·mol(Hf)⁻¹·h⁻¹·atm⁻¹ at 70 °C (entry 17 in Table 1). In general, the hafnium procatalyst **5** showed lower activity than its zirconium analogue **4** did. In both catalytic systems of zirconium and hafnium, the catalytic activities were greatly improved with an increase of ethylene pressure, which were consistent with our former observations because higher ethylene pressure enhanced the coordination and insertion of ethylene for fast polymerization.^{8d,27} The obtained PEs possessed melting points in the range 133–136 °C, typical for high-density polyethylene (HDPE). The *T_m* and *M_w* values

(22) (a) Gade, L. H.; Memmler, H.; Kauper, U.; Schneider, A.; Fabre, S.; Bezougli, I.; Lutz, M.; Galka, C.; Scowen, I. J.; McPartlin, M. *Chem.—Eur. J.* **2000**, *6*, 692. (b) Memmler, H.; Walsh, K.; Gade, L. H. *Inorg. Chem.* **1995**, *34*, 4062.

(23) Shafir, A.; Arnold, J. *Organometallics* **2003**, *22*, 567.

(24) Zhang, Y. H.; Kissunko, D. A.; Fettingner, J. C.; Sita, L. R. *Organometallics* **2003**, *22*, 21.

(25) Ramos, C.; Royo, P.; Lanfranchi, M.; Pellinghelli, M. A.; Tiripicchio, A. *Eur. J. Inorg. Chem.* **2005**, 3962.

(26) Gauvin, R. M.; Lorber, C.; Choukroun, R.; Donnadieu, B.; Kress, J. *Eur. J. Inorg. Chem.* **2001**, 2337.

(27) (a) Zuo, W.; Zhang, M.; Sun, W.-H. *J. Polym. Sci., Part A: Polym. Chem.* **2009**, *47*, 357. (b) Zhang, S.; Sun, W.-H.; Xiao, T.; Hao, X. *Organometallics* **2010**, *29*, 1168.

Table 1. Ethylene Polymerization with Procatalysts 4 and 5^e

entry	procat.	cocat.	<i>P</i> (atm)	<i>T</i> (°C)	Al/ <i>M</i> ^a	activity ^b	<i>T</i> _m (°C) ^c	<i>M</i> _w ^d	<i>M</i> _w / <i>M</i> _n ^d
1	4	Et ₂ AlCl	1	30	200	trace			
2	4	AlEt ₃	1	30	200	trace			
3	4	MMAO	1	30	1000	1.30	135.3	6.18	56
4	4	MAO	1	30	1000	2.10	135.1		
5	4	MAO	1	50	1000	2.70	134.1	3.37	15
6	4	MAO	1	70	1000	0.80	133.3		
7	4	MAO	10	30	500	5.26	135.5		
8	4	MAO	10	30	1000	5.92	134.9	16.7	8.2
9	4	MAO	10	30	1500	4.43	133.5		
10	4	MAO	10	50	1000	7.21	134.6	9.07	13
11	4	MAO	10	60	1000	10.6	134.2	4.20	9.1
12	4	MAO	10	70	1000	17.3	133.7	3.37	8.7
13	4	MAO	10	80	1000	13.8	133.2		
14	5	MAO	10	30	1000	0.23	135.7	13.0	24
15	5	MAO	10	50	1000	0.83	135.2	8.12	21
16	5	MAO	10	60	1000	1.05	134.8		
17	5	MAO	10	70	1000	2.40	134.7	4.21	15
18	5	MAO	10	80	1000	0.96	134.5		

^a*M* = Zr or Hf. ^b10⁴ g·mol(M)⁻¹·h⁻¹·atm⁻¹. ^cDetermined by DSC. ^d10⁵ g·mol⁻¹. Determined by GPC. ^eConditions: 5 μmol of procat., 30 min; total volume: 30 mL of toluene at 1 atm or 100 mL of toluene at 10 atm.

Table 2. Ethylene Polymerization with Procatalysts 2/MAO and 6/MAO^d

entry	procat.	<i>P</i> (atm)	<i>T</i> (°C)	Al/Zr	activity ^a	<i>T</i> _m (°C) ^b	<i>M</i> _w ^c	<i>M</i> _w / <i>M</i> _n ^c
1	2	1	50	1000	trace			
2	2	10	30	1000	2.96	135.8	5.43	4.9
3	2	10	50	500	2.65	135.6		
4	2	10	50	1000	3.36	135.0		
5	2	10	50	1500	2.84	133.1	2.22	4.6
6	2	10	60	1000	5.00	133.8		
7	2	10	70	1000	6.92	133.3	2.53	4.2
8	2	10	80	1000	4.32	133.1		
9	6	1	30	1000	trace			
10	6	1	50	1000	0.80	133.8	4.72	65
11	6	1	70	1000	trace			
12	6	10	30	1000	2.84	135.4	6.37	24
13	6	10	50	1000	4.52	135.1	6.12	13
14	6	10	60	1000	6.68	134.8		
15	6	10	70	1000	9.76	134.2	4.11	11
16	6	10	80	1000	5.96	133.8		

^a10⁴ g·mol(Zr)⁻¹·h⁻¹·atm⁻¹. ^bDetermined by DSC. ^c10⁵ g·mol⁻¹. Determined by GPC. ^dConditions: 5 μmol of Zr, 30 min; total volume: 30 mL of toluene at 1 atm of ethylene or 100 mL of toluene at 10 atm of ethylene.

of PEs gradually decreased with an increase in the reaction temperature (entries 1–18 in Table 1).

The procatalysts **2** and **6** were investigated in parallel in the presence of MAO, and their results were tabulated in Table 2. In a comparison with results by procatalyst **4**, both procatalysts **2** and **6** showed relatively lower activities for ethylene polymerization. Varying the reaction conditions (entries 1–8 for procatalyst **2** and entries 9–16 for procatalyst **6** in Table 2), the optimum condition was the 1000 Al/Zr molar ratios under 10 atm of ethylene at 70 °C with the highest activity of 6.92 × 10⁴ g·mol(Zr)⁻¹·h⁻¹·atm⁻¹ by **2** (entry 7 in Table 2) and 9.76 × 10⁴ g·mol(Zr)⁻¹·h⁻¹·atm⁻¹ by **6** (entry 15 in Table 2), respectively. Given that the only difference between compounds **3** and **4** is the coordinated solvent (THF vs Et₂O), procatalyst **3** was not investigated because it was believed to create the same active zirconium species as its analogue **4**.

In all cases, the best activities were observed with the 1000 Al/Zr molar ratio under 10 atm of ethylene at 70 °C. In order to reduce viscosity of the solution and improve mass transportation at elevated temperatures, the procatalysts should be activated at 70 °C. Such temperatures are favored for commercially applicable catalysts (about 80 °C for the

Ziegler–Natta catalytic system). The resultant PEs have high molecular weights; for example, with the 1000 Al/Zr molar ratios under 10 atm of ethylene at 30 °C, procatalyst **4** produced PE with the molecular weight 1670 kg·mol⁻¹ (entry 8 in Table 1), while PE by **2** showed a molecular weight of 543 kg·mol⁻¹ (entry 2 in Table 2), 1300 kg·mol⁻¹ for PE by **5** (entry 14 in Table 1), and 637 kg·mol⁻¹ for PE by **6** (entry 12 in Table 2). Moreover, the resultant PEs have broader molecular weight distributions at lower reaction temperature, indicating that uniform formation of active sites requires higher reaction temperatures. Since the polymerization is a highly exothermic reaction, the reaction temperature will rise and accelerate the formation of the active species.

Although the ethylene polymerization was conducted in a homogeneous catalytic system, the resultant PEs showed broad molecular weight distributions (4.2–65) (Tables 1 and 2). Regarding zirconium procatalysts, procatalyst **2** produced PE with a low molecular weight and narrow molecular weight distribution, while **4** produced PE with the highest molecular weight but slightly broader polydispersity, and **6** gave PE with moderate molecular weight and even wider molecular distribution. In complex **2**, there are two

Table 3. Ethylene/1-Hexene Copolymerization with Procatalysts 2/MAO and 6/MAO^d

entry	procatal.	<i>T</i> (°C)	activity ^a	<i>T</i> _m (°C) ^b	<i>M</i> _w ^c	<i>M</i> _w / <i>M</i> _n ^c
1	2	30	3.84	130.9		
2	2	60	6.98	129.8	6.07	17
3	2	70	8.28	129.1	3.39	16
4	2	80	6.28	128.6		
5	6	30	4.84	130.5		
6	6	60	9.68	129.2	10.6	33
7	6	70	10.3	128.6	3.34	26
8	6	80	8.96	127.3		

^a 10⁴ g·mol(Zr)⁻¹·h⁻¹·atm⁻¹. ^b Determined by DSC. ^c 10⁵ g·mol⁻¹. Determined by GPC. ^d Conditions: 5 μmol of Zr, 30 min, Al/Zr = 1000; total volume: 100 mL of toluene at 10 atm.

μ_2, η^1 -*N*-[(*N,N*-dimethylamino)dimethylsilyl]-2,6-diisopropylanilidates occupying spaces around zirconium; therefore the active species is likely to be uniform, giving PEs with narrow *M*_w/*M*_n. On the other hand, a bulky environment surrounding active zirconium caused slow coordination of ethylene and potentially terminated chain growth, so the PEs obtained by **2** had low molecular weights. It is likely that the LiCl adduct is removed when forming its active species of procatalyst **4** with zirconium coordinated with one μ_2, η^1 -*N*-[(*N,N*-dimethylamino)dimethylsilyl]-2,6-diisopropylanilidate, which provided more space for monomer coordination and resulted in PEs showing high molecular weights. In comparison with **2**, procatalyst **4** seems to form a less stable active species, and although a higher activity was observed for **4**, multiple active sites were formed, leading to PEs with wide molecular weight distributions. However, the PEs by **6** have wider molecular distributions with molecular weights between PEs by procatalysts **2** and **4**.^{28,29} Procatalyst **6**, being symmetrically split, is likely to provide the same active sites as **2**, which produced PEs with high molecular weights; beyond that, dimeric active sites and other mononuclear active sites may be responsible for PEs with different molecular weights. This would result in PE samples produced with **6** showing wide molecular weight distributions, which is observed.

Ethylene/1-Hexene Copolymerization. Regarding the high performance of branched polyolefins,^{27a,29} the copolymerizations of ethylene/1-hexene by **2**/MAO and **6**/MAO were successfully carried out, and the results are illustrated in Table 3. At 10 atm of ethylene pressure, with the Al/Zr molar ratio of 1000 and 1-hexene (6 mL), the catalytic reactions were monitored at different temperatures for procatalysts **2** (entries 1–4 in Table 3) and **6** (entries 5–8 in Table 3). The copolymerization activity is higher than those observed in homopolymerization of ethylene (Table 2). The best active values are obtained at 70 °C in the range 20 to 80 °C: 8.28 × 10⁵ g·mol(Zr)⁻¹·h⁻¹·atm⁻¹ for the procatalyst **2** (entry 3 in Table 3) and 1.03 × 10⁵ g·mol(Zr)⁻¹·h⁻¹·atm⁻¹ for the procatalyst **6** (entry 7 in Table 3). The introduction of 1-hexene produces butyl branches, which results in lower melting points (127–131 °C) than linear polyethylene. Both *T*_m and *M*_w

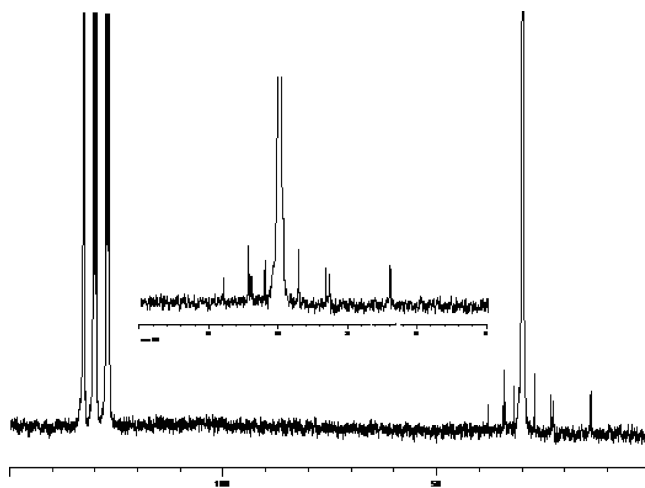


Figure 6. ¹³C NMR spectrum of poly(ethylene-co-1-hexene) prepared by **6**/MAO (entry 7 in Table 3).

values of the copolymers decrease gradually with the reaction temperatures (entries 1–8 in Table 3), while the copolymers' molecular weight distributions are broader than polymers in homopolymerization. Again, copolymers by **2** showed narrow molecular distributions. Changing copolymerization parameters and using a different procatalyst, the molecular weights and weight distributions of copolymers obtained could be controlled.

¹³C NMR analysis of the resultant poly(ethylene-co-1-hexene) revealed a ¹³C NMR spectrum of butyl-branched polyethylene, indicating a typical linear low-density polyethylene (LLDPE).³⁰ It showed about 3% branched carbon incorporated polymer resulted from **6**/MAO (Figure 6).

Summary

The new lithium μ_2, η^1 -*N*-[(*N,N*-dimethylamino)dimethylsilyl]-2,6-diisopropylanilidate dimer (**1c**) and the μ_2, η^1 -*N*-[(*N,N*-dimethylamino)dimethylsilyl]-2,6-diisopropylanilidometal (zirconium or hafnium) procatalysts **2–6** are synthesized and characterized. The procatalysts **2** and **4–6** showed good activity toward ethylene polymerization (up to 1.73 × 10⁵ g·mol(Zr)⁻¹·h⁻¹·atm⁻¹) and gave PEs with broad molecular weight distributions. Procatalyst **2**, containing two ligands, produced polymers with relatively narrow molecular weight distributions because of better stability of its active species, while procatalyst **4**, bearing one ligand, showed high activity and produced polymers with high molecular weights but wider molecular weight distributions. The dimeric procatalyst **6** apparently provides multiple active species and produces polymers with wider molecular weight distributions. In the copolymerization of ethylene with 1-hexene, the resultant copolymers indicated nice incorporation of 1-hexene, and these procatalysts are promising for further investigation. More importantly, the current zirconium procatalysts exhibited excellent thermal stability at 70 °C regarding the aspect of industrial requirement.

(28) (a) Vollmerhaus, R.; Rahim, M.; Tomaszewski, R.; Xin, S.; Taylor, N. J.; Collins, S. *Organometallics* **2000**, *19*, 2161. (b) Xie, G.; Qian, C. *J. Polym. Sci., Part A: Polym. Chem.* **2008**, *46*, 211. (c) Kim, W. K.; Fevola, M. J.; Liable-Sands, L. M.; Rheingold, A. L.; Theopold, K. H. *Organometallics* **1998**, *17*, 4541.

(29) (a) Hong, H.; Zhang, Z.; Chung, T. C.; Lee, R. W. *J. Polym. Sci., Part A: Polym. Chem.* **2007**, *45*, 639. (b) Smit, M.; Zheng, X.; Loos, J.; Chadwick, J. C.; Koning, C. E. *J. Polym. Sci., Part A: Polym. Chem.* **2006**, *44*, 6652.

(30) (a) Yano, A.; Gasegawa, S.; Kaneko, T.; Sone, M.; Sato, M.; Akimoto, A. *Macromol. Chem. Phys.* **1999**, *200*, 1542. (b) Quijada, R.; Galland, G. B.; Mauler, R. S.; de Menezes, S. C. *Macromol. Rapid Commun.* **1996**, *17*, 607. (c) Chu, K.-J.; Soares, J. B. P.; Penlidis, A. *Macromol. Chem. Phys.* **2000**, *201*, 340. (d) Zhang, Y.; Yang, X.; Yu, Y.; Qian, Y.; Huang, J. *Chin. J. Chem.* **2005**, *23*, 1081. (e) Czaja, K.; Bialek, M. *Polymer* **2001**, *42*, 2289.

Experimental Section

General Procedures. All manipulations were carried out under an atmosphere of argon using standard Schlenk techniques. Deuterated solvents C_6D_6 and $CDCl_3$ were dried over activated molecular sieves (4 Å) and vacuum transferred before use. Hexane was dried over sodium potassium alloy. Diethyl ether was dried and distilled from sodium/benzophenone and stored over a sodium mirror under argon. Dichloromethane was distilled from activated molecular sieves (4 Å). Toluene was refluxed in the presence of sodium/benzophenone and distilled under nitrogen prior to use. The NMR spectra were recorded on a Bruker DKX-300 spectrometer with TMS as the internal standard. Elemental analyses were performed with a Flash EA 1112 microanalyzer. The polymerization-grade ethylene was supplied by Beijing Yansan Petrochemical Co. Et_2AlCl (1.90 M in toluene) and $AlEt_3$ (2.0 M in hexane) were purchased from Acros Chemicals, while methylaluminoxane (MAO, 1.46 M in toluene) and modified methylaluminoxane (MMAO, 1.93 M in heptane) were purchased from Ablemarle Corp. ^{13}C NMR spectra of the copolymers were recorded on a Bruker DMX-300 MHz instrument at 135 °C in deuterated 1,2-dichlorobenzene with TMS as an internal standard. The GPC curves were obtained by plotting detector response versus elution volume using polystyrene standards (with an approximate polydispersity index). Further fractionalization of fractions was not performed. Melting points of polyolefins were measured on a Perkin-Elmer DSC-7 differential scanning calorimetry (DSC) analyzer. Under a nitrogen atmosphere, a sample of about 2.0–6.0 mg was heated from 50 to 160 °C at a rate of 10 °C/min and kept for 5 min at 160 °C to remove the thermal history, then cooled at a rate of 10 °C/min to 50 °C. The DSC trace and the melting points of the samples were obtained from the second scanning run.

Lithium μ_2 -2,6-Diisopropylhydridoanilidoanilidate Dimer Ether Adduct ($[(2,6\text{-}^iPr_2C_6H_3)HNLi \cdot Et_2O]_2$, **1a**). To a solution of 2,6-diisopropylbenzenamine (2.0 mL, 10 mmol) in 25 mL of Et_2O at 0 °C was added dropwise $nBuLi$ (3.50 mL, 2.86 M, 10 mmol) to form a colorless solution. The mixture was warmed to room temperature and kept stirring for 6 h. Hexane (25 mL) was layered on the solution to obtain the product **1a** (2.48 g) in 97% yield as colorless crystals. 1H NMR (300 MHz C_6D_6): δ 1.04–1.09 (t, 6H, CH_3 , Et_2O), 1.22, 1.26 (q, 12H, $^3J_{HH} = 6.9$ Hz, $CH(CH_3)_2$), 1.45 (s, 1H, NH), 2.94–2.98 (m, 2H, $CH(CH_3)_2$), 3.21–3.28 (m, 4H, CH_2 , Et_2O), 6.86 (m, 1H, *p*-Ph), 7.20–7.22 (m, 2H, *o,m*-Ph). ^{13}C NMR (75 MHz C_6D_6): δ 15.96 (CH_3 , Et_2O), 23.92, 24.29 ($CH(CH_3)_2$), 28.14, 29.24 ($CH(CH_3)_2$), 66.53 (CH_2 , Et_2O), 112.61, 119.73, 123.82, 124.35, 132.74, 156.92 (Ph).

$N-[(N,N\text{-Dimethylamino})dimethylsilyl]-2,6\text{-diisopropylaniline}$ ($(CH_3)_2N(CH_3)_2SiNH(2,6\text{-}^iPr_2C_6H_3)$ as **HL**, **1b**). To a solution of **1a** (2.54 g, 5 mmol) in 25 mL of hexane at 0 °C was dropwise transferred Me_2NMe_2SiCl (1.49 mL, 10 mmol) to form a colorless solution, which gradually turned to a white, cloudy solution. The mixture was warmed to room temperature and stirred for 12 h. The resulting white residue was filtered, and the filtrate was concentrated. Oily compound **1b** was formed (2.78 g) in 98% yield. Attempts to purify the product by extraction with hexanes were unsuccessful because of the high solubility of the yellow oil in all these solvents. 1H NMR (300 MHz $CDCl_3$): δ 0.13 (s, 6H, $Si(CH_3)_2$), 1.18, 1.20 (d, 12H, $^3J_{HH} = 6.9$ Hz, $CH(CH_3)_2$), 2.52 (s, 6H, $N(CH_3)_2$), 3.34–3.41 (m, 2H, $CH(CH_3)_2$), 6.95–6.99 (m, 1H, *p*-Ph), 7.04–7.09 (m, 2H, *o,m*-Ph).

Lithium $\mu_2\eta^1-N-[(N,N\text{-Dimethylamino})dimethylsilyl]-2,6\text{-diisopropylanilidate Dimer}$ ($[Li(CH_3)_2N(CH_3)_2SiN(2,6\text{-}^iPr_2C_6H_3)]_2$ as **(LiL)₂**, **1c**). To a solution of **1b** (0.59 g, 2 mmol) in 25 mL of THF at 0 °C was dropwise added $nBuLi$ (0.7 mL, 2.86 M, 2 mmol) to form a colorless solution, which gradually disappeared and changed to a yellow solution. The mixture was warmed to room temperature and kept stirring for 12 h. Then 25 mL of hexane

was layered on the yellow solution to obtain the product **1c** (0.55 g) in 97% isolated yield as colorless crystals. 1H NMR (300 MHz C_6D_6): δ 0.38 (s, 6H, $Si(CH_3)_2$), 1.34, 1.49 (q, 12H, $^3J_{HH} = 6.0$ Hz, $CH(CH_3)_2$), 2.46 (s, 6H, $N(CH_3)_2$), 3.87 (m, 2H, $CH(CH_3)_2$), 7.32–7.35 (m, 2H, *m*-Ph), 7.42 (m, 1H, *p*-Ph). ^{13}C NMR (75 MHz C_6D_6): δ -0.08 ($Si(CH_3)_2$), 24.04, 25.14 ($CH(CH_3)_2$), 27.33 ($CH(CH_3)_2$), 40.08 ($N(CH_3)_2$), 119.23 (*p*-Ph), 122.99, 123.63 (*m*-Ph), 142.66 (*o*-Ph), 148.66 (*ipso*- C_{Ph}).

Bis($\mu_2\eta^1-N-[(N,N\text{-dimethylamino})dimethylsilyl]-2,6\text{-diisopropylanilido}$)zirconium Dichloride [ZrL_2Cl_2 , **2**]. To a solution of **1c** (0.57 g, 1 mmol) in 25 mL of THF at -78 °C was added $ZrCl_4$ (0.23 g, 1 mmol). The resulting mixture was stirred for a while, then warmed to room temperature and kept stirring for 24 h. Volatile compounds were removed *in vacuo*, and the resulting residue was extracted with toluene and filtered. The filtrate was concentrated *in vacuo* to ca. 10 mL. The compound **2** was crystallized at -20 °C as colorless crystals (0.49 g) in 69% yield. Mp: 57–58 °C (dec). Anal. Calcd for $C_{32}H_{58}Cl_2N_4Si_2Zr$: C, 53.53; H, 8.09; N, 7.84. Found: C, 53.50; H, 8.12; N, 7.86. 1H NMR (300 MHz $CDCl_3$): δ 0.39–0.66 (d, 12H, $Si(CH_3)_2$), 1.11, 1.24 (m, 24H, $^3J_{HH} = 6.6$ Hz, $CH(CH_3)_2$), 3.59 (m, 4H, $CH(CH_3)_2$), 2.80–3.02 (d, 12H, $N(CH_3)_2$), 6.97–7.01 (m, 4H, *m*-Ph), 7.09–7.11 (m, 2H, *p*-Ph). ^{13}C NMR (75 MHz $CDCl_3$): δ 3.55 ($Si(CH_3)_2$), 22.50, 23.09, 23.44, 24.29, 24.71, 25.11, 25.42, 25.67 ($CH(CH_3)_2$), 26.26, 26.93, 36.49, 41.46 ($CH(CH_3)_2$), 43.90, 45.09 ($N(CH_3)_2$), 121.78, 122.49 (*p*-Ph), 122.88, 123.18 (*m*-Ph), 140.50, 141.54, 142.47, 145.31 (*ipso*- C_{Ph}).

$\mu_2\eta^1-N-[(N,N\text{-Dimethylamino})dimethylsilyl]-2,6\text{-diisopropylanilidozirconium Chloride-Lithium Chloride THF Adduct}$ [$ZrLCl_2(\mu\text{-Cl})_2Li \cdot 2THF$, **3**]. Using a similar procedure to that for **2** but with equimolar reactants of lithium and zirconium, the resultant residue was extracted with toluene and filtered. The filtrate was dried *in vacuo* and dissolved in a mixture of toluene and THF (4:1) at -10 °C to obtain compound **3** as red crystals (1.03 g) in 78% yield. Mp: 149–151 °C (dec). Anal. Calcd for $C_{24}H_{43}Cl_4LiN_2O_2SiZr$: C, 43.52; H, 6.80; N, 4.28. Found: C, 43.46; H, 6.82; N, 4.31. 1H NMR (300 MHz $CDCl_3$): δ 0.36 (s, 6H, $Si(CH_3)_2$), 1.17, 1.27 (q, 12H, $^3J_{HH} = 6.3$ Hz, $CH(CH_3)_2$), 1.89 (s, 8H, THF), 2.33 (m, 2H, $^3J_{HH} = 6.3$ Hz, $CH(CH_3)_2$), 2.90 (s, 6H, $N(CH_3)_2$), 3.90 (s, 8H, THF), 7.03–7.23 (m, 3H, Ph). ^{13}C NMR (75 MHz $CDCl_3$): δ 1.56 ($Si(CH_3)_2$), 27.06, 28.16 ($CH(CH_3)_2$), 29.45 ($CH(CH_3)_2$), 30.02 (THF), 49.07 ($N(CH_3)_2$), 72.30 (THF), 127.97 (*p*-Ph), 131.34 (*m*-Ph), 145.43, 147.80 (*ipso*- C_{Ph}).

$\mu_2\eta^1-N-[(N,N\text{-Dimethylamino})dimethylsilyl]-2,6\text{-diisopropylanilidozirconium Chloride-Lithium Chloride Ether Adduct}$ [$ZrLCl_2(\mu\text{-Cl})_2Li \cdot 2Et_2O$, **4**]. The same procedure as the synthesis of compound **3** was used; however, its product was dissolved in ether and crystallized to give yellow crystals of compound **4** (0.84 g) in 63% yield. Mp: 82–83 °C (dec). Anal. Calcd for $C_{24}H_{49}Cl_4LiN_2O_2SiZr$: C, 43.26; H, 7.36; N, 4.23. Found: C, 43.23; H, 7.34; N, 4.27. 1H NMR (300 MHz $CDCl_3$): δ 0.17 (s, 6H, $Si(CH_3)_2$), 1.01 (d, 12H, $^3J_{HH} = 7.2$ Hz, $CH(CH_3)_2$), 1.23 (s, 12H, Et_2O), 2.71 (s, 6H, $N(CH_3)_2$), 3.32 (s, 8H, Et_2O), 3.63 (m, 2H, $CH(CH_3)_2$), 6.87 (m, 3H, Ph). ^{13}C NMR (75 MHz $CDCl_3$): δ -0.09 ($Si(CH_3)_2$), 25.25, 28.27 ($CH(CH_3)_2$), 27.75, 28.69 ($CH(CH_3)_2$), 46.88 ($N(CH_3)_2$), 124.86 (*p*-Ph), 125.16 (*m*-Ph), 143.49, 146.25 (*ipso*- C_{Ph}).

$\mu_2\eta^1-N-[(N,N\text{-Dimethylamino})dimethylsilyl]-2,6\text{-diisopropylanilidohafnium Chloride-Lithium Chloride Ether Adduct}$ [$HfLCl_2(\mu\text{-Cl})_2Li \cdot 2Et_2O$, **5**]. Using the same procedure of synthesis as compound **3**, with hafnium chloride instead of zirconium chloride, light yellow crystals of compound **5** (0.89 g, 59% yield) were obtained from its ether solution. Mp: 63–64 °C (dec). Anal. Calcd for $C_{24}H_{49}Cl_4LiN_2O_2SiHf$: C, 38.25; H, 6.51; N, 3.72. Found: C, 38.21; H, 6.53; N, 3.76. 1H NMR (300 MHz $CDCl_3$): δ 0.37 (s, 6H, $Si(CH_3)_2$), 1.20 (d, 12H, $^3J_{HH} = 7.2$ Hz, $CH(CH_3)_2$), 1.27 (t, 12H, $^3J_{HH} = 6.6$ Hz, Et_2O), 2.97 (s, 6H, $N(CH_3)_2$), 3.50 (q, 8H, $^3J_{HH} = 6.9$ Hz, Et_2O), 3.92 (m, 2H, $CH(CH_3)_2$), 7.08 (m, 1H, *p*-Ph), 7.11 (m, 2H, *m*-Ph). ^{13}C NMR (75 MHz $CDCl_3$): δ -0.09 ($Si(CH_3)_2$), 24.57 ($CH(CH_3)_2$), 27.24 ($CH(CH_3)_2$), 46.48 ($N(CH_3)_2$), 123.75 (*o*-Ph), 144.17 (*ipso*- C_{Ph}).

μ_2, η^1 -*N*-[(*N,N*-Dimethylamino)dimethylsilyl]-2,6-diisopropylani-
lidozirconium Chloride Dimer $\{[\text{ZrLCl}_2(\mu\text{-Cl})_2]_2, \mathbf{6}\}$. The same
procedure as the synthesis of compound **3** was used; however,
its product was dissolved in dichloromethane and crystallized at
−10 °C to give yellow crystals of compound **6** (0.77 g) in 81%
yield. Mp: 52–53 °C (dec). Anal. Calcd for $\text{C}_{32}\text{H}_{58}\text{Cl}_6\text{N}_4\text{Si}_2\text{Zr}_2$:
C, 40.68; H, 6.14; N, 5.93. Found: C, 40.71; H, 6.12; N, 5.90. ^1H
NMR (300 MHz CDCl_3): δ 0.10 (s, 6H, $\text{Si}(\text{CH}_3)_2$), 1.12 (d, 12H,
 $^3J_{\text{HH}} = 7.2$ Hz, $\text{CH}(\text{CH}_3)_2$), 3.34 (m, 2H, $\text{CH}(\text{CH}_3)_2$), 2.06 (s, 6H,
 $\text{N}(\text{CH}_3)_2$), 6.65 (m, 3H, Ph). ^{13}C NMR (75 MHz CDCl_3): δ −0.01
($\text{Si}(\text{CH}_3)_2$), 25.54, 28.69 ($\text{CH}(\text{CH}_3)_2$), 27.51, 28.88 ($\text{CH}(\text{CH}_3)_2$),
46.78 ($\text{N}(\text{CH}_3)_2$), 124.60 (*p*-Ph), 125.57 (*m*-Ph), 143.47, 146.51
(*ipso*- C_{Ph}).

**Procedures for Ethylene Polymerization. Polymerization at 1
atm of Pressure.** The metal compound (5 μmol) was added to a
Schlenk-type flask under nitrogen. This flask was backfilled
three times with nitrogen and twice with ethylene, then charged
with the required amount of freshly distilled toluene. At the
chosen temperature, the reaction solution was vigorously stirred
under 1 atm of ethylene for the desired period of time after
adding the desired amount of MAO solution. The polymeriza-
tion reaction was quenched by adding 10% HCl–ethanol solu-
tion (60 mL), and then the mixture was poured into 100 mL of
ethanol to precipitate the polymer, which was further washed
with ethanol and water followed by drying under vacuum at
60 °C to its constant weight. In the case of ethylene/1-hexene
copolymerization, 1-hexene (dried with calcium hydride) in
toluene was added prior to the addition of MAO.

Polymerization at 10 atm of Pressure. For polymerization at
higher ethylene pressure, a stainless steel autoclave (0.5 L
capacity) equipped with gas ballast through a solenoid valve
for continuous feeding of ethylene at constant pressure was
used. The autoclave was heated under vacuum to over 80 °C and

recharged with ethylene three times, then cooled to room
temperature. A toluene solution of the catalysts (and monomer)
was transferred to the reactor, which was then maintained at
the desired temperature. MAO solution to give a final volume of
100 mL was then added to start the polymerization; then the
autoclave was immediately pressurized to the desired pressure.
After 30 min, the autoclave was placed in a water–ice bath for
an hour, then opened with adding 10% HCl–acidic ethanol.
The solid polyolefin was washed with ethanol and water several
times and then dried under vacuum to constant weight.

X-ray Crystallography. Data collection of **1a**, **1c**, and **2–6** was
performed with Mo K α radiation ($\lambda = 0.71073$ Å) on a Bruker
Smart Apex CCD diffractometer at 173(2) or 213(2) K. Crystals
were coated in oil and then directly mounted on the diffrac-
tometer under a stream of cold nitrogen gas. A total of *N*
reflections were collected by using the ω scan mode. Intensities
were corrected for Lorentz and polarization effects and empiri-
cal absorption. The structures were solved by direct methods and
refined by full-matrix least-squares on F^2 . All non-hydrogen
atoms were refined anisotropically. Structure solution and refine-
ment were performed by using the SHELXL-97 package.³¹
Crystal data collection and refinement details for all compounds
are available in Table S8 of the Supporting Information.

Acknowledgment. We thank the Natural Science Foun-
dation of China (20772074 and 20874105) and SXNSF
(2008011021 and 2008012013-2).

Supporting Information Available: The GPC diagrams of
corresponding polyolefins, molecular structures of compounds
4 and **5**, bond lengths and angles of compounds **1a**, **1c**, and **2–6**,
crystal data and processing parameters for compounds **1a**, **1c**,
and **2–6**, and a CIF file giving crystallographic data. This
material is available free of charge via the Internet at <http://pubs.acs.org>.

(31) Sheldrick, G. M. *SHELXL-97, Program for the Solution of
Crystal Structures*; University of Göttingen: Göttingen, Germany, 1997.